Grasping and In-Hand Manipulation: Experiments with a Reconfigurable Gripper

Attawith Sudsang, Jean Ponce and Narayan Srinivasa
Beckman Institute, University of Illinois, Urbana, IL 61801

Abstract

This paper addresses the problem of grasping and manipulating three-dimensional objects with a reconfigurable gripper equipped with two parallel plates whose distance can be adjusted by a computer-controlled actuator. The bottom plate is a bare plane, and the top one carries a rectangular grid of actuated pins that can translate in discrete increments under computer control. We propose to use this gripper to immobilize objects through frictionless contacts with three of the pins and the bottom plate, and to manipulate an object within a grasp by planning the sequence of pin configurations that will bring this object to a desired position and orientation. A detailed analysis of the problem geometry in configuration space was used in [44] to devise simple and efficient algorithms for grasp and manipulation planning. We have constructed a prototype of the gripper and this paper presents our experiments.

1 Introduction

When a hand holds an object at rest, the forces and moments exerted by the fingers should balance each other so as not to disturb the position of this object. We say that such a grasp achieves *equilibrium*. For the hand to hold the object securely, it should also be capable of preventing any motion due

to external forces and torques. Since screw theory [2, 13, 26] can be used to represented both displacements (*twists*) and forces and moments (*wrenches*), it is an appropriate tool for analyzing and synthesizing grasps. Indeed, it is known that six independent contact wrenches are necessary to prevent any infinitesimal displacement which maintains contact, and that a seventh one is required to ensure that contact cannot be broken [14, 41]. Such a grasp prevents any infinitesimal motion of the object, and it is said to achieve *form closure* [26, 34, 40]. A system of wrenches is said to achieve *force closure* when it can balance any external force and torque. Like wrenches and infinitesimal twists [39], force and form closure are dual notions and, as noted in [24, 25] for example, force closure implies form closure and vice versa.

The notions of form and force closure are the traditional theoretical basis for grasp planning algorithms. Mishra, Schwartz, and Sharir [23] have proposed linear-time algorithms for computing a finger configuration achieving force closure for frictionless polyhedral objects. Markenscoff and Papadimitriou [19] and Mirtich and Canny [21] have proposed algorithms for planning grasps which are optimal according to various criteria [10]. In each of these works, the grasp-planning algorithm outputs a single grasp for a given set of contact faces. Assuming Coulomb friction [25], Nguyen has proposed instead a geometric method for computing *maximal independent* two-finger grasps of polygons, i.e., segments of the polygonal boundary where the two fingers can be positioned independently while maintaining force closure, requiring

as little positional accuracy from the robot as possible. This approach has been generalized to handle various numbers of fingers and different object geometries in [3, 7, 27, 29, 30, 31]

Recently, Rimon and Burdick have introduced the notion of *second-order immobility* [36, 37, 38] and shown that certain equilibrium grasps (or fixtures) of a part which do not achieve form closure effectively prevent any *finite* motion of this part through curvature effects in configuration space. They have given operational conditions for immobilization and proven the dynamic stability of immobilizing grasps under various deformation models [38]. An additional advantage of their theory is that second-order immobilization can be achieved with fewer fingers (four contacts for convex fingers) than form closure (seven contacts [14, 41]).

In [45, 42, 44], we introduced a new approach to grasp and manipulation planning based on the notion of second-order immobility and a detailed analysis of the geometric constraints imposed by object/finger contacts in configuration space. This approach applies to a new class of reconfigurabe grippers with mostly discrete degrees of freedom (Figure 1), and it is related to recent work in modular fixture planning [4, 5, 22, 47, 48, 46] and to a number of sensorless pushing and squeezing manipulation algorithms [1, 9, 12, 18, 20, 33, 35]. Indeed, the class of devices we are interested in can be seen as automatically reconfigurable fixtures, but since they are capable of both immobilizing a part and manipulating it within a grasp, we will

continue in the rest of this paper to call them grippers.

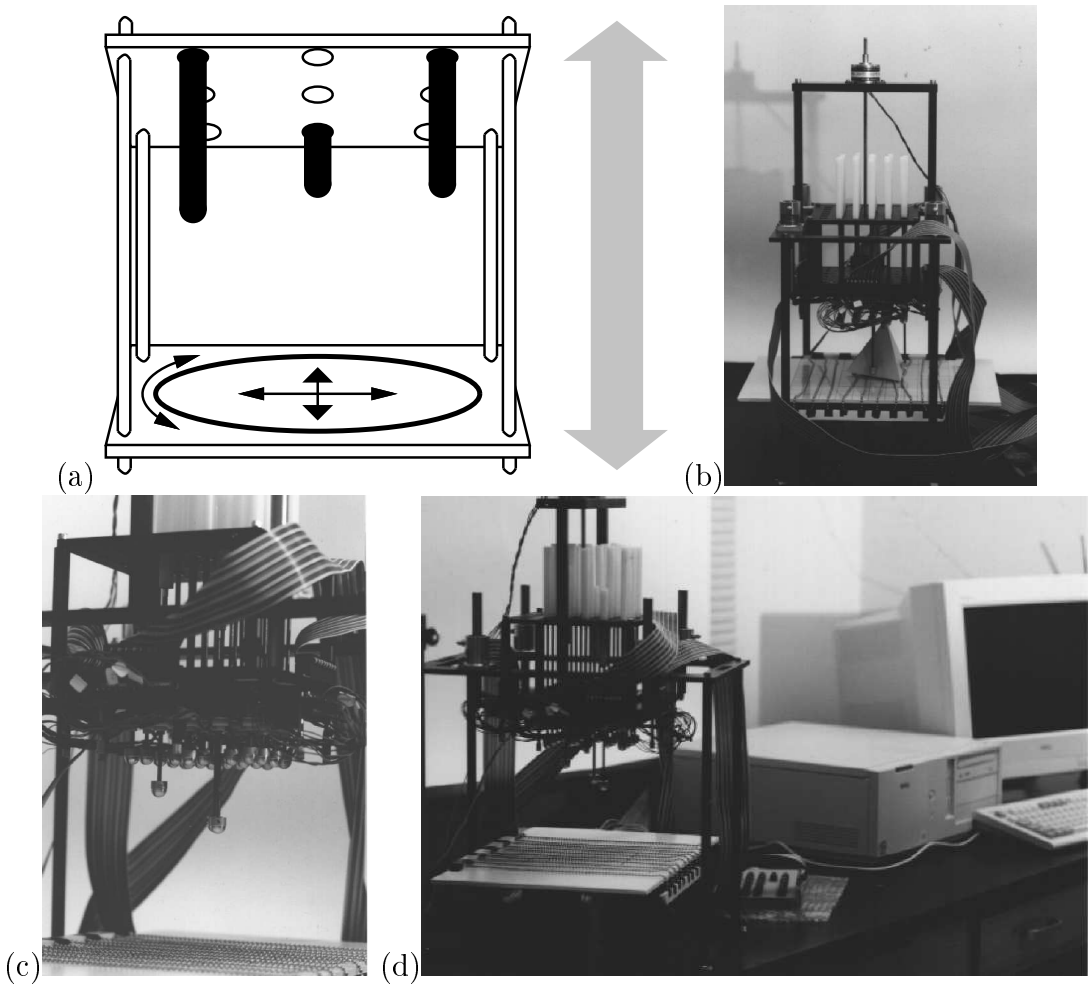

Figure 1: A reconfigurable gripper: (a) conceptual design and (b)-(d) actual prototype.

Figure 1(a) shows the conceptual design of the proposed device: it is equipped with two parallel plates whose distance can be adjusted by a computer-controlled actuator. The bottom plate is a bare plane, and the top one carries

a rectangular grid of actuated pins that can translate in discrete increments under computer control. We have developed efficient algorithms for planning grasps and in-hand manipulation tasks for this gripper in the companion papers [45, 42, 44]. Since then, we have completed the construction of a prototype of the gripper, and this paper, after briefly recalling the principles of our planning algorithms, focusses on our experiments with this prototype.

Figure 1(b)-(d) shows some pictures of our prototype: it is equipped with a grid of twenty five fingers, each one of them being mounted on the lead screw of a separate linear actuator. The top and lower plate assemblies can be moved relative to each other using a large linear actuator. To avoid friction as much as possible, the bottom plate is covered with a series of strings of metal beads, which lets the manipulated part roll with minimal resistance. We should stress that designs that are simpler, more reliable and more accurate, are of course possible: for example, we only need three pins to move at any time, which does not require one actuator per pin. Our main goal here is to demonstrate that manipulation tasks can actually be performed using our approach, and the current gripper design is only for proof-of-concept experiments such as the ones described in the latter sections of this paper. We plan to refine this design and construct a second prototype in the months to come.

2 Grasp Planning

In this section, we address the problem of grasping a three-dimensional polyhedral object with the reconfigurable gripper shown in Figure 1. We derive geometric conditions for contact, equilibrium, and immobility. We then use these conditions in a simple and efficient algorithm for enumerating all immobilizing grasps of a polyhedral object. Here as in the rest of this paper, we assume hard-finger frictionless contact, so each pin exerts a pure force on the grasped object at the point of contact. The force $\boldsymbol{f}$ exerted at the point $\boldsymbol{p}$ and its moment can be represented by the *zero-pitch wrench* [2, 13, 26]

$$\boldsymbol{w} = \begin{pmatrix} \boldsymbol{f} \\ \boldsymbol{p} \times \boldsymbol{f} \end{pmatrix},$$

where "$\times$" denotes the operator that associates to two vectors their cross-product.

The validity of the frictionless assumption in real robotics systems is discussed in [44], and it is investigated in the experiments described later in the paper.

2.1 Geometry of the Problem

Our gripper can be used to hold a polyhedral object through contacts with three of the top plate pins, and either a face, an edge-and-vertex, or a three-vertex contact with the bottom plate. Let us assume for the sake of simplicity that the faces of the polyhedron are triangular (as shown in [45, 44], our

approach can in fact handle arbitrary convex polygons). Any wrench exerted at a contact point between a face and the bottom plate can be written as a positive combination of wrenches at the vertices. Likewise, the wrenches corresponding to an edge-and-vertex contact are positive combinations of wrenches exerted at the end-points of the line segment and at the vertex.

We detail the case of a contact between the bottom plate and a triangular face f with inward normal $\boldsymbol{n}$ and vertices $\boldsymbol{v}_i$ $(i = 1, 2, 3)$ and denote by f_i $(i = 1, 2, 3)$ the remaining faces, with inward normals $\boldsymbol{n}_i$ (Figure 2).

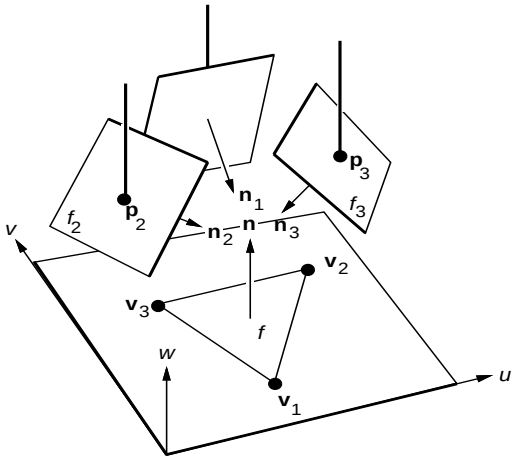

Figure 2: The four faces involved in a grasp.

We also assume without loss of generality that the four vectors $\boldsymbol{n}$ and $\boldsymbol{n}_i$ $(i = 1, 2, 3)$ *positively span* $\mathbb{R}^3$, i.e., that a strictly positive linear combination of these vectors is equal to zero (this is a necessary condition for essential equilibrium). Finally, given the physical layout of our gripper, contact between the upper-jaw pins and faces such that $\boldsymbol{n} \cdot \boldsymbol{n}_i > 0$ is of course

impossible, and we further assume without loss of generality that $\boldsymbol{n} \cdot \boldsymbol{n}_i < 0$ for $i = 1, 2, 3$.

Under these assumptions, we can choose a coordinate system (u, v, w) attached to the object with w axis parallel to $\boldsymbol{n}$, and write in this coordinate system $\boldsymbol{n} = (0, 0, 1)^T$ and $\boldsymbol{n}_i = (a_i, b_i, -1)^T$ (note that $\boldsymbol{n}_i$ is not a unit vector).

Likewise, since the vectors $\boldsymbol{n}$ and $\boldsymbol{n}_i$ $(i = 1, 2, 3)$ positively span $\mathbb{R}^3$, we can write $\boldsymbol{n} = -\sum_{i=1}^{3} \mu_i \boldsymbol{n}_i$, where $\mu_i > 0$ for $i = 1, 2, 3$. To complete the specification of the faces f_i $(i = 1, 2, 3)$, we will denote by c_i the height of f_i at the origin, so the plane of this face can be parameterized by $w_i = a_i u_i + b_i v_i + c_i$. Finally, since the faces f_i are convex, the fact that the point associated with the parameters u_i, v_i actually belongs to f_i can be expressed by three linear inequalities on u_i, v_i (these will be referred to as *face bounds inequalities* in the sequel).

2.1.1 Contact

We reduce the problem of achieving contact between a spherical pin and a plane to the problem of achieving point contact with a plane. This is done without loss of generality by growing the object to be fixtured by the pin radius and shrinking the spherical end of the pin into its center (see [6, 47, 48] for a similar approach in the two-dimensional case). We attach a coordinate system (q, r, w) to the gripper, and denote by $\mathcal{R}$ and $\boldsymbol{t}$ the rotation of angle

θ about $\boldsymbol{n}$ and the translation (x, y) in the plane orthogonal to $\boldsymbol{n}$ that map the (q, r, w) coordinate system onto the (u, v, w) coordinate system.

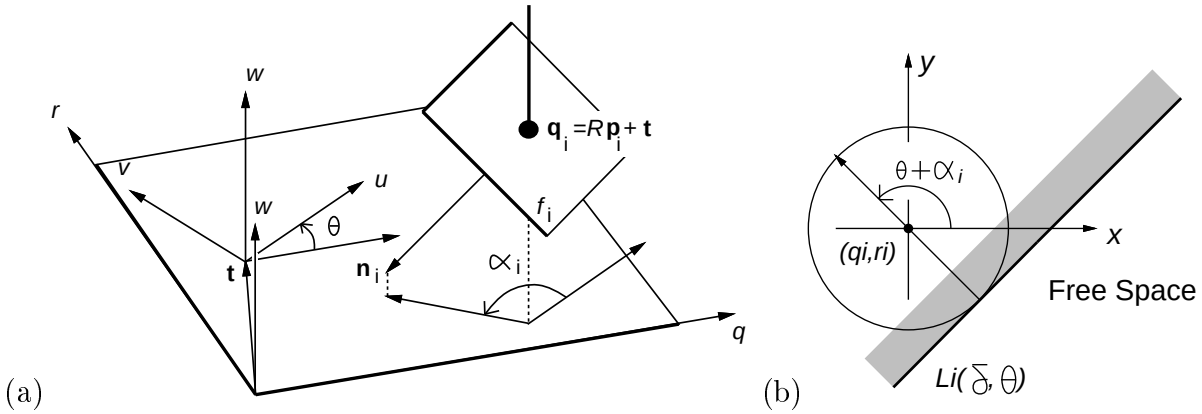

Figure 3: Contact between a pin and a face: (a) in the workspace; (b) in configuration space.

If $\boldsymbol{p}_i$ and $\boldsymbol{q}_i$ denote respectively the positions of the tip of pin number i in the object's and gripper's coordinate frames, we can write $\boldsymbol{p}_i = (u_i, v_i, a_i u_i + b_i v_i + c_i)^T$, $\boldsymbol{q}_i = (q_i, r_i, \delta - h_i)$ and $\boldsymbol{q}_i = \mathcal{R}\boldsymbol{p}_i + \boldsymbol{t}$, where q_i, r_i and h_i denote respectively the integer pin position on the bottom plate grid and its height, and δ is the jaw separation.

This change of coordinates yields a condition for contact between pin number i and the corresponding face. It can be rewritten as an equation $\mathcal{C}_i(x, y, \theta, \delta) = 0$ which, for given values of δ and θ, defines a straight line $L_i(\delta, \theta)$ in the (x, y) plane (Figure 3(b)). As θ changes, this line rotates around the point (q_i, r_i), the angle between the x axis and its normal being $\theta + \alpha_i$, where α_i is simply the angle between the u axis and the projection

of $\boldsymbol{n}_i$ onto the u, v plane (Figure 3(a)). The distance between the point (q_i, r_i) and the line varies as a linear function of δ and the height h_i of the corresponding pin.

For a given jaw separation δ, the set $S_i(\delta)$ of object configurations (x, y, θ) for which $\mathcal{C}_i(x, y, \theta, \delta) = 0$ forms a ruled surface, which is one of the surfaces bounding the corresponding configuration space obstacle [17].

The three pins will be in contact with the corresponding faces when the corresponding contact equations are satisfied. Eliminating the variables x and y among these equations yields

$$\mathcal{E}(\delta, \theta) \stackrel{\text{def}}{=} \delta - A\cos(\theta - \alpha) - B = 0, \tag{1}$$

where A and B are linear functions of the pin positions and height, but α depends only on the pins' position but not their heights [44]. It follows that a necessary condition for the existence of an object position achieving contact with the three pins is that the point (θ, δ) lies on the *contact sinusoid* defined by $\mathcal{E}(\delta, \theta) = 0$. This condition is also sufficient: for given values of θ and δ on this sinusoid, the three linear equations $\mathcal{C}_i(x, y, \theta, \delta) = 0$ $(i = 1, 2, 3)$ in the two unknowns x and y are linearly dependent, and thus admit a common solution.

2.1.2 Equilibrium

In general, given d frictionless contacts between points $\boldsymbol{p}_i$ and faces f_i with internal normals $\boldsymbol{n}_i$ $(i = 1, .., d)$, equilibrium is achieved when the contact

wrenches balance each other, i.e., $\sum_{i=1}^{d} \lambda_i(\boldsymbol{n}_i, \boldsymbol{p}_i \times \boldsymbol{n}_i) = 0$ for some $\lambda_i \geq 0$ $(i = 1, .., d)$ with $\sum_{i=1}^{d} \lambda_i = 1$ (note that the value of a wrench depends on the choice of origin, but that the condition for equilibrium does not). Equilibrium is a necessary, but not sufficient, condition for immobility.

The equilibrium equation expresses both force and moment equilibrium. In our setting, force equilibrium is a simple condition on the surface normals. Combining it with the moment equilibrium equation and the change of coordinates used earlier yields, after some simple algebraic manipulation, $\sin(\theta - \alpha) = 0$. It follows that a necessary condition for three pins in contact with the corresponding faces of the object to achieve equilibrium is that $\theta = \alpha$ or $\theta = \alpha + \pi$. Note that these values of θ are independent of the heights of the pins, which will prove extremely important in the grasp planning algorithm presented in Section 2.2. Note that this condition is just necessary. To check that a given grasp configuration actually achieves equilibrium, we compute the values of the coefficients λ_i for $i = 1, 2, 3$. If they are all positive, then equilibrium is achieved.

2.1.3 Immobility

Rimon and Burdick have formalized the notion of immobilizing grasps in terms of isolated points of the free configuration space [36, 37, 38] (see also related work by Czyzowicz, Stojmenovic and Urrutia [8] and Mirtich and Canny [21]). They have shown that equilibrium grasps that do not achieve

form closure may still immobilize an object through second-order (curvature) effects in configuration space: a sufficient condition for immobility is that the *relative curvature form* associated with an essential equilibrium grasp or fixture be negative definite (essential equilibrium is achieved when the coefficients λ_i in the equilibrium equation are uniquely defined and strictly positive [37]). The relative curvature form can be computed in terms of the contact positions as well as the surface normals and curvatures of the body and pins at the contacts.

In the case of equilibrium contacts between pins with a spherical tip and polyhedra, it is easily shown [28] that the symmetric matrix associated with the relative curvature form is

$$\mathcal{K} = \sum_{i=1}^{d} \lambda_i \{([\boldsymbol{n}_{i\times}]^T[\boldsymbol{p}_{i\times}])^S - r_i[\boldsymbol{n}_{i\times}]^T[\boldsymbol{n}_{i\times}]\}, \tag{2}$$

where r_i denotes the pin's radius, the weights λ_i are the weights used in the equilibrium equation, and, by definition, $\mathcal{A}^S = \frac{1}{2}(\mathcal{A} + \mathcal{A}^T)$. (Note that this formula assumes *unit* normals: this it must be adjusted for our formulation.)

In the case of our gripper, the radii corresponding to the planar contacts are effectively infinite, and it is obvious that $\boldsymbol{\omega}^T\mathcal{K}\boldsymbol{\omega}$ is negative for any vector $\boldsymbol{\omega}$ which is not parallel to $\boldsymbol{n}$. Thus we must determine the sign of $\boldsymbol{n}^T\mathcal{K}\boldsymbol{n}$, whose value is easily shown to be $AM\cos(\theta - \alpha)$, where M is a normalizing positive constant balancing the fact that we are not using unit normals. It follows that $\mathcal{K}$ is negative definite if and only if $\theta = \alpha + \pi$.

2.1.4 Main Result

We can now summarize the results obtained in this section with the following lemma.

Lemma 1: For given integer pin positions and heights q_i, r_i and h_i ($i = 1, 2, 3$), a sufficient condition for an object at configuration (x_0, y_0, θ_0) to be immobilized by a grasp with jaw separation δ_0 is that:

(1) $\theta_0 = \alpha + \pi$,

(2) $\mathcal{C}_i(x_0, y_0, \theta_0, \delta_0) = 0$ for $i = 1, 2, 3$,

(3) if $\mathcal{R}_0$ denotes the rotation of angle θ_0 about $\boldsymbol{n}$, and $\boldsymbol{t}_0$ denotes the translation (x_0, y_0), the points $\mathcal{R}_0(\boldsymbol{q}_i - \boldsymbol{t}_0)$ satisfy the face bounds inequalities for $i = 1, 2, 3$, and

(4) the equilibrium constraints on the coefficients λ_i ($i = 1, 2, 3$) admit a positive solution.

This lemma is an obvious corollary of the results obtained in the previous sections, the third condition simply expressing the fact that the contacts must occur within the faces.

2.2 Algorithm

According to Lemma 1, all continuous degrees of freedom of a grasp (object orientation, jaw separation and object position) can be computed once the

grasp's discrete degrees of freedom (pin positions and heights) have been set. This yields the following naive algorithm for grasp planning: for each quadruple of faces, enumerate all grid positions and heights of the three pins, then compute the remaining grasp parameters and check whether they satisfy conditions (3) and (4) of Lemma 1. The complexity of this algorithm is obviously $O(N^4 D^6)$, where N is the number of faces of the grasped polyhedron, and D is its diameter measured in units equal to the distance between successive grid points.

A better approach is the following algorithm, which has the same overall structure as the naive one, but limits the number of faces and gripper configurations under consideration by exploiting a number of geometric constraints, most notably the fact that the orientation of an object held in an immobilizing grasp depends only on the pins' positions and not on their heights:

For each quadruple of faces do

(1) Test whether they can be held in equilibrium.

(2) Enumerate all pin positions that may hold the object in equilibrium and compute the corresponding object orientation.

(3) For each such position, enumerate the pin lengths that immobilize the object and compute the remaining grasp parameters.

(4) Compute the corresponding coefficients λ_i and check that they are positive.

In the first step of the algorithm, we only consider quadruples of faces whose normals positively span $\mathbb{R}^3$. For these faces, the equilibrium constraints provide four linear equations in the the nine unknowns λ_i, u_i, v_i $(i = 1, 2, 3)$, and the existence of equilibrium configurations can be tested by using linear programming to determine whether the five-dimensional polytope defined by these constraints and the face bounds inequalities and $\lambda_i \geq 0$ is empty. When this polytope is not empty, the subset of each face that may participate in an equilibrium configuration is efficiently determined using polytope projection techniques [11, 16, 15, 31] (see [45, 44] for details).

The second step of our algorithm uses distance constraints to reduce the enumeration of the pin positions that may yield equilibrium grasps to the scan-line conversion of circular shells (see [4, 5, 47, 48] for related approaches to fixture planning for two-dimensional objects): clearly each pin must lie within the horizontal projection of each face. Thus, if we position the first pin at the origin, the integer point corresponding to the second pin is constrained to lie within the circular shell centered at the origin with inner radius equal to the minimum distance between the projections of the two corresponding faces and outer radius equal to the maximum distance. Given the position of the second pin, the third pin is now constrained to lie within the region formed by the intersection of the two shells associated with the first and

second pin. Enumerating the pin locations thus amounts to determining the integer positions falling in planar regions defined by a circular shell or the intersection of two such shells. This is done in optimal time proportional to the number of these points by using a scan-line conversion algorithm (Figure 4).

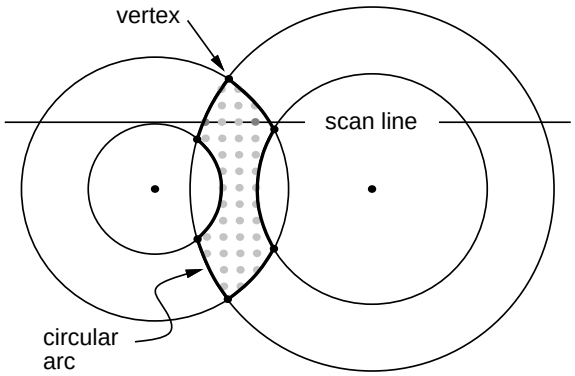

Figure 4: Scan-line conversion: spans between consecutive boundary elements are filled one scan-line at a time.

The third step of the algorithm uses condition (3) of Lemma 1 to reduce the enumeration of pin heights that yield immobilizing grasps to polygon scan conversion. Once the position of the pins has been chosen and the corresponding rotation has been computed, we can align the gripper's and object's coordinate systems so they are only separated by the horizontal translation (x, y). This allows us to rewrite the contact equations as linear equations in x, y, δ and the heights h_i $(i = 1, 2, 3)$ of the pins.

In turn, writing that the pins actually lie within the bounds of the associated faces constrains the possible values of x and y: in particular, if

f_i' the convex polygon constructed by projecting f_i onto the (u_i, v_i) plane, then applying to the projection a symmetry with respect to the origin and a translation by (q_i, r_i)), it is easy to show using the contact equations that the point (x, y) is restricted to lie within the polygon $F' = f_1' \cap f_2' \cap f_3'$ (Figure 5(a)). Using this constraint, the contact equation, and the fact that we can position the first pin at the origin with zero length, it follows that (h_2, h_3) is restricted to lie in a second convex polygon, obtained from F' via an affine transformation [42, 44]. These points can once again be determined in optimal time proportional to their actual number using a polygon scan-line conversion algorithm.

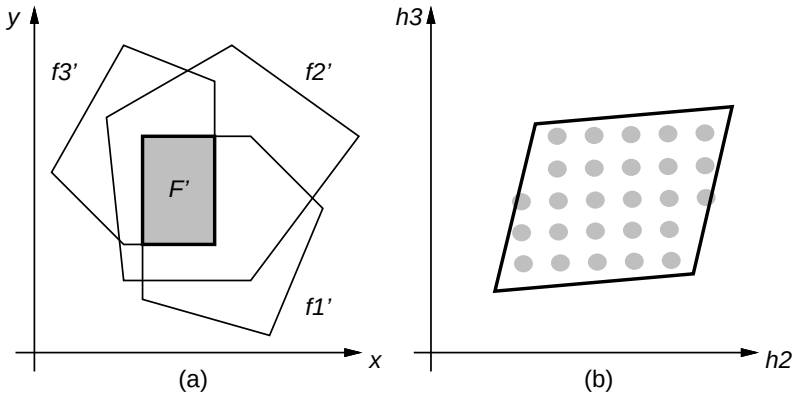

Figure 5: Enumerating pin lengths: (a) the polygon F' defined in the x, y plane by the intersection of the faces f_i', and (b) the corresponding convex polygon in the h_2, h_3 plane, along with the integer points inside it.

Now, for a given configuration (location plus height) of the pins, the contact equations forms a system of three linear equations in the three variables x, y, and δ. This system is readily solved to yield the pose of the object and

the separation of the plates. The values of the coefficients λ_i are easily computed at this point, and step (4) of the algorithm checks that these values are positive and indeed define an equilibrium grasp.

As shown in [45, 44], the overall time complexity of the algorithm is $O(N^4D^2d^4)$ where d is the maximum diameter of the object's faces (note that $d \leq D$, and that for polyhedra with many faces having roughly the same area, d is in general much smaller than D).

3 In-Hand Manipulation

We now present an approach to in-hand manipulation based on the concept of *inescapable configuration space* (ICS) region , i.e., on the idea of characterizing the regions of configuration space for which the object is not immobilized but is constrained to lie within a bounded region of the free configuration space (see [35] for related work in the two-dimensional, two-finger case).

ICS regions allow us to plan in-hand object motions as sequences of gripper configurations (see [1, 9, 12, 18, 20, 33, 35] for related work): starting from some immobilizing configuration, we can open the gripper jaws and retract the immobilizing pins, then choose another triple of pins whose ICS region contains the initial gripper configuration, lower these pins, and as the jaws close, move the object to the corresponding immobilized configuration. Note that this approach does not require modeling what happens when contact occurs, but it indeed requires frictionless contacts to avoid wedging.

We will assume in the rest of this section that the quadruple of faces under consideration is fixed.

3.1 Geometry of the Problem

3.1.1 Free Configuration Space Regions

Let us consider an immobilizing configuration of the gripper, defined by the position q_i, r_i and height h_i of the pins ($i = 1, 2, 3$), by the position x_0, y_0 and orientation θ_0 of the object in the gripper's coordinate system, and by the jaw separation δ_0. We assume that the values of q_i, r_i and h_i are held constant and examine what happens when the separation of the jaws changes.

The ruled surface $S_i(\delta)$ defined earlier splits the three-dimensional space $\mathbb{R}^2 \times S^1$ of configurations x, y, θ into a "free" half-space $V_i(\delta)$ and a "forbidden" half-space $W_i(\delta)$ where pin number i penetrates the plane of f_i. Furthermore, $V_i(\delta)$ (resp. $W_i(\delta)$) is characterized by $\mathcal{C}_i(x, y, \theta, \delta) \geq 0$ (resp. ≤ 0).

Now let us consider the volume $V(\delta) = V_1(\delta) \cap V_2(\delta) \cap V_3(\delta)$. Given the form of $C_i(x, y, \theta, \delta)$, it is obvious that if a configuration lies in free space for some value δ_1 of δ, it also lies in free space for any other value $\delta_2 \geq \delta_1$. In other words, $V(\delta_1) \subset V(\delta_2)$ when $\delta_2 \geq \delta_1$ (this is also intuitively obvious since increasing δ corresponds to opening the jaws). In particular, the immobilizing configuration (x_0, y_0, θ_0) is always in free space for $\delta \geq \delta_0$.

The intersection of $V(\delta)$ with a plane $\theta =$ constant forms a triangular

region $T(\delta, \theta)$. Note that the triangles corresponding to various values of θ are all homothetic since their edges make constant angles with each other. However, their size, position, and orientation varies with θ. It is easy to show that these triangles, although possibly empty, are not degenerate [42, 44].

As shown in Figure 6, the region $T(\delta, \theta)$ may contain an open subset (Figure 6(a)), be reduced to a single point (Figure 6(b)), or be empty (Figure 6(c)).

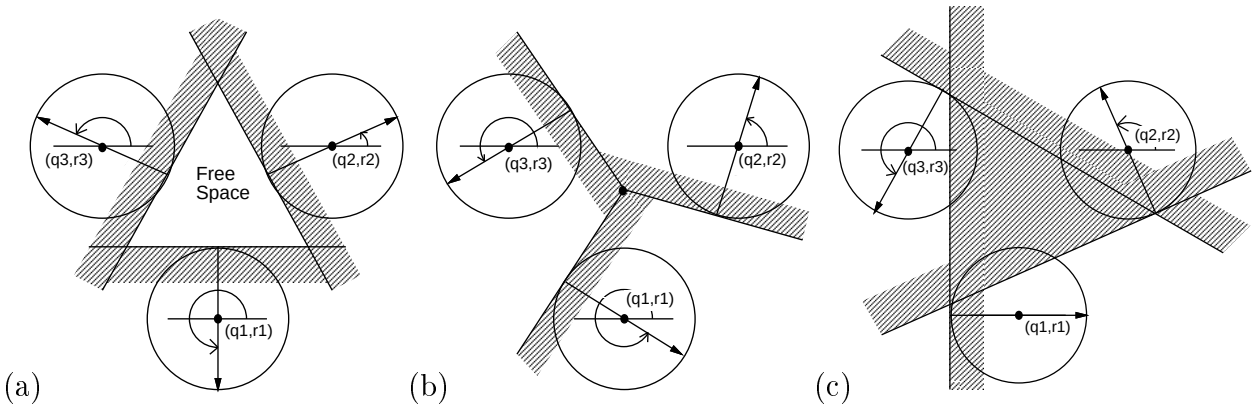

Figure 6: Possible configurations of the intersection $T(\delta, \theta)$ of $V(\delta)$ with a plane θ = constant: (a) $T(\delta, \theta)$ contains an open neighborhood; (b) it is reduced to an isolated point of the x, y plane; (c) it is empty.

In the second case (Figure 6(b)), the three pins simultaneously touch the corresponding faces, and $\mathcal{E}(\delta, \theta) = 0$. In fact, it is easy to show that a necessary and sufficient condition for $T(\delta, \theta)$ to contain at least one point is that $\mathcal{E}(\delta, \theta) \geq 0$ [42, 44]. This allows us to characterize qualitatively the range of orientations θ for which $T(\delta, \theta)$ is not empty (Figure 7): for a given δ, the condition $\mathcal{E}(\delta, \theta) = 0$ is an equation in θ that may have zero, one,

or two real solutions: a double root occurs at the minimum $\delta = \delta_0$ or at the maximum $\delta = \delta_{\max}$ of the sinusoid. In the former case, $\mathcal{E}$ is strictly positive everywhere except at $\theta = \alpha$ where it is equal to zero, and the range of orientations is S^1. In the latter case, the range of orientations reduces to a single point $\theta_0 = \alpha + \pi$. For any value δ_1 in the open interval $]\delta_0, \delta_{\max}[$, there are two distinct roots θ', θ'', and the range of orientations is the arc bounded by these roots and containing θ_0. Finally, for values of δ outside the $[\delta_0, \delta_{\max}]$ interval, there is no solution: either δ is strictly smaller than δ_0 and the range of orientations is empty (at least one of the pins penetrates the plane of the corresponding face), or δ is strictly larger than $\delta_{\max}$, and the range of orientations is S^1.

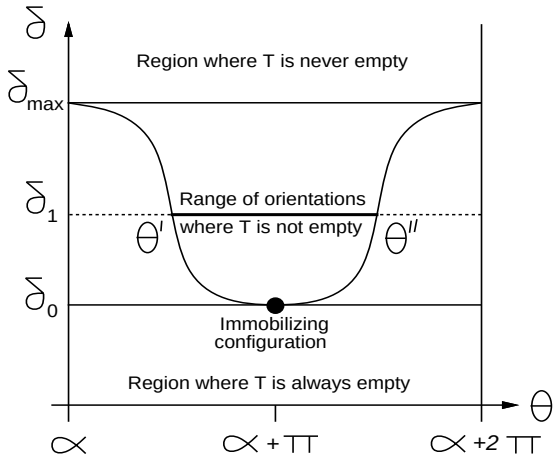

Figure 7: Regions of θ, δ space delimited by the sinusoid $\mathcal{E}(\delta, \theta) = 0$.

In particular, since the volume $V(\delta)$ is a stack of contiguous triangles $T(\delta, \theta)$, it is clear at this point that, for $\delta \geq \delta_0$, $V(\delta)$ is a non-empty, con-

nected, compact region of $\mathbb{R}^2 \times S^1$. The analysis conducted in this section also gives some geometric insight on the immobility conditions derived earlier. In particular, it confirms that the minimum point $(\alpha + \pi, \delta_0)$ of the contact sinusoid corresponds to an isolated point of configuration space or equivalently to an immobilizing configuration: indeed, the triangle $T(\delta_0, \alpha + \pi)$ is reduced to a point, and $T(\delta, \theta)$ is empty for any $\theta \neq \theta_0$. Likewise, although the maximum $(\alpha, \delta_{\max})$ of the sinusoid corresponds to an equilibrium grasp, it does not yield an immobilizing grasp since the object is free to undergo arbitrary rotations.

3.1.2 Inescapable Configuration Space Regions

The discussion so far has characterized the contacts between the pins and the planes of the corresponding faces, ignoring the fact that each face is in fact a convex polygon in its plane. Let us consider the set $E_i(\delta, \theta)$ of configurations (x, y) for which the tip of pin number i belongs to the corresponding face. Obviously, $E_i(\delta, \theta)$ is a subset of $L_i(\delta, \theta)$. It is easy to show by combining the contact equation with the corresponding face bounds equations that $E_i(\delta, \theta)$ is a line segment, and that the location of its endpoints along the line $L_i(\delta, \theta)$ is a piecewise-linear function of δ.

Now let us consider the three segments $E_i(\delta, \theta)$ $(i = 1, 2, 3)$ together (Figure 8): if $E_i(\delta, \theta)$ and $E_j(\delta, \theta)$ intersect for all $i \neq j$, then the three segments completely enclose the triangle $T(\delta, \theta)$ (Figure 8(a)). We say that

the corresponding configuration satisfies the *enclosure condition* since there is no escape path for the object in the x, y plane with the corresponding orientation θ. More generally, when all triples of segments in the range of orientations associated with a given jaw separation δ satisfy the enclosure condition, $V(\delta)$ itself is an *inescapable configuration space* (ICS) region: in other words, the object is free to move within the region $V(\delta)$, but remains imprisoned by the grasp and cannot escape to infinity.

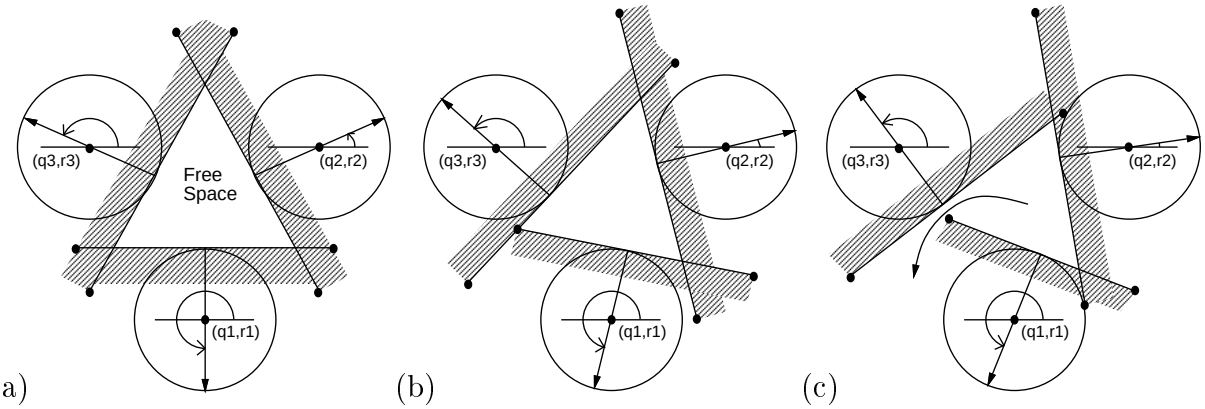

(a) (b) (c)

Figure 8: Triangle configurations: (a) three segments enclosing a triangle; (b) a critical configuration; (c) an opened triangle and an escape path.

3.1.3 Maximum ICS Regions

Here we address the problem of characterizing the maximum value δ^* for which $V(\delta)$ forms an ICS region for any δ in the $[\delta_0, \delta^*]$ interval. We know that at $\delta = \delta_0$ the three segments intersect at the immobilizing configuration, forming an ICS region reduced to a single point. Thus the enclosure condition holds at $\delta = \delta_0$. On the other hand, as $\delta \to +\infty$, the whole configuration

space becomes free of obstacles, thus there must exist a critical point for some minimal value of δ greater than δ_0. This guarantees that δ^* has a finite value.

As shown by Figure 8(b), a critical event occurs when one of the endpoints of a segment lies on the line supporting another segment. After this event, the line segments fail to enclose the triangle $T(\delta, \theta)$ and the object can escape the grasp (Figure 8(c)).

A critical event occurs when the endpoint under consideration is on the line $L_j(\delta, \theta)$ for some $j \neq i$. Algebraically, this is easily written as

$$A_{ij} \cos(\theta + \beta_{ij}) + B_{ij}\delta + C_{ij} = 0, \tag{3}$$

where A_{ij}, B_{ij} and C_{ij} are appropriate constants given in [42, 44].

In other words, critical configurations form a second sinusoid in θ, δ space, called the *critical sinusoid* in the rest of this presentation.

We seek the minimum value of $\delta^* > \delta_0$ for which the range of orientations includes one of the critical orientations. As discussed above, we know that δ^* exists. Let us suppose first that a critical value lies in the interior of the range of orientations associated with some $\delta_1 \geq \delta_0$, and denote by $\delta_{\min}$ the minimum value of δ on the critical sinusoid. By definition, we have $\delta_1 \geq \delta_{\min}$. Suppose that $\delta_1 > \delta_{\min}$. Then by continuity, there exists some δ_2 such that $\delta_{\min} < \delta_2 < \delta_1$ and the corresponding range of orientations also contains a critical orientation (Figure 9). The argument holds for any value of $\delta > \delta_{\min}$.

In other words, either the range of orientations of $\delta_{\min}$ contains a critical orientation, in which case $\delta^* = \delta_{\min}$ (Figure 9(a)), or it does not, in which case the critical value associated with δ^* must be one of its range's endpoints (Figure 9(b)). This is checked by intersecting the contact sinusoid and the critical one. Note that this process must be repeated six times (once per each segment/vertex pair) to select the minimum value of δ^*.

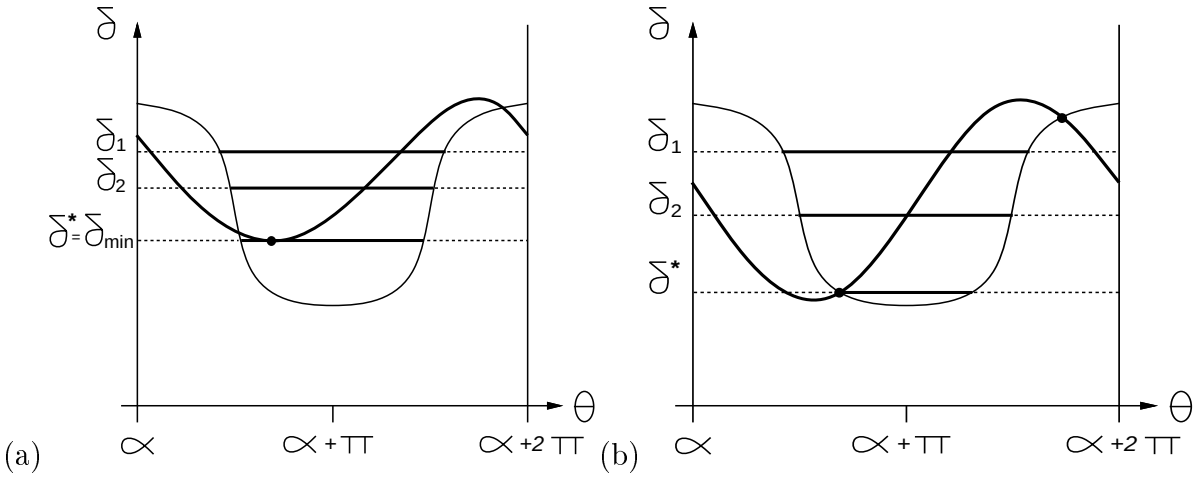

Figure 9: Critical configurations: (a) the critical configuration is the minimum of the critical sinusoid (shown as the thicker curve); (b) the critical configuration is the minimum intersection of the critical sinusoid and the contact sinusoid.

3.1.4 Main Result

The following lemma follows immediately from the results established in Sections 3.1.1, 3.1.2 and 3.1.3 and summarizes the findings of these sections.

Lemma 2: For given integer pin positions and heights q_i, r_i and h_i ($i = 1, 2, 3$) and an immobilizing configuration $(x_0, y_0, \theta_0, \delta_0)$, there exists a critical

jaw separation δ^* such that:

(1) for any $\delta > \delta^*$, there exists a path allowing the object to escape the grasp,

(2) for any δ in the interval $[\delta_0, \delta^*]$, the volume $V(\delta)$ is an inescapable region of configuration space that contains the configuration $(x_0, y_0, \theta_0, \delta_0)$,

(3) for any $\delta' \leq \delta''$ in the interval $[\delta_0, \delta^*]$, $V(\delta') \subset V(\delta'')$, and

(4) δ^* can be computed in closed form as the minimum of a sinusoid or the intersection of two sinusoids.

3.2 Algorithm

Lemma 2 can be used as a basis for in-hand manipulation by remarking that an object anywhere in the ICS region associated with some gripper configuration can be moved to the corresponding immobilized position and orientation by closing the gripper jaws (this follows immediately from properties (2) and (3) in Lemma 2). Thus we can plan manipulation sequences from one immobilized configuration to another by using the following algorithm.

Off-line:

(1) Compute the set S of all immobilizing configurations of the object.

(2) Construct a directed graph G whose vertices are the elements of S and whose edges are the pairs (s, s') of elements of S such that s belongs to the maximum ICS region $\mathrm{ICS}(s')$ associated with s'.

On-line:

(3) Given two configurations i and g in S, search the graph G for the shortest path going from the initial configuration i to the goal configuration g.

Once a path has been found, the corresponding manipulation sequence can be executed: starting from the configuration i, each edge (s, s') in the path allows us to move the object from s to s' by opening the jaws and retracting the pins associated with s, then lowering the pins associated with s' and closing the jaws.

The grasp planning algorithm of Section 2 can of course be used to implement Step (1) of the algorithm. Finding "all" immobilizing configurations has, however, slightly different meanings in manipulation and grasping tasks: during grasp planning, one can always assume that the first pin is at the origin with zero height. Of course, when a grasp is actually executed, the pin positions and heights, along with the jaw separation, all have to be shifted so that the corresponding variables are all positive and the pin positions remain within the extent of the top plate. Nonetheless, gripper configurations that only differ by a shift of the three pin positions are equivalent for grasping

purposes. This is not the case for in-hand manipulation, where the goal is to move the object held by the gripper across the bottom plate: this forces us to take into account all shifted configurations of a grasp.

We will say that a triple of pin positions with the first pin located at the origin is a *prototype*, and that all positions of the triple within the bottom plate are the *shifts* of this prototype. For each prototype, we can define the minimum rectangle aligned with the (p, q) coordinate axes and enclosing the pins. If W and H denote the width and height of this rectangle, and K^2 is the total number of grid elements, the prototype admits $(K - W)(K - H)$ different shifts, which can trivially be computed in time proportional to their number. As shown in [42, 44], there are $O(D^2d^2)$ immobilizing prototypes, to which correspond $O(D^2d^4K^2)$ shifted object/gripper configurations. If we assume that the manipulated object fits completely on the gripper's bottom plate, note that we will have $d \leq D \leq K$.

Deciding whether an immobilizing configuration s belongs to the maximum ICS region of another configuration s' does not require an explicit boundary representation of ICS(s'): it is sufficient to test whether s belongs to the triangle associated with s' at the corresponding immobilizing orientation. In addition, as shown in [42, 44], the construction of G in Step (3) of our algorithm can be implemented efficiently by mapping it onto a *three-dimensional dominance* problem [32]. Finally, Step (4) can be implemented as a breadth-first search of the graph G. The overall time complexity of the

algorithm is dominated by the cost of the graph construction, which is easily shown to be $O(P^2d^2K^2 \log K + V + E)$, where V denotes the number of immobilizing gripper configurations (or equivalently the number of vertices of G), P denotes the number of prototypes associated with these configurations, and E is the number of edges of G [42, 44]. Note that $P = O(D^2d^2)$, $V = O(Pd^2K^2)$, and $E = O(V^2)$.

4 Implementation and Results

We have implemented the grasp and manipulation planning algorithms in C, and used our gripper prototype to test their performance in actual robotic tasks. The program runs on Sun SparcStation 10. For the experiment given here, it takes 3 seconds to compute all grasps, and 147 seconds to construct the graph for manipulation planning. This section describes our experiments. Extensive simulation results can be found in the companion paper [44].

4.1 Friction

All contacts must be kept as close to frictionless as possible. Strands of metal beads are used to lessen the frictional resistance between the bottom plate and the object. The friction between the pin tips and the object also need to be considered, and we smoothed the surface of the pin tips. This is important because jamming may cause the pins to bend instead of letting the object reach the desired configuration.

4.2 Gripper Calibration

To correctly operate, the gripper requires calibration. The calibration has two parts. First, we need to calibrate the large actuator that controls the height of the plate. This is currently performed by manually measuring the actual height of the plate, and passing this parameter to the computer that will command the actuator to a prespecified home position. Once the plate is at the correct home position, we continue with the second part of the calibration. We place a level metal board under the top plate, and keep actuating all the small motors that control the pins until the tips hit the board. Clearly, the height of all pins are now equal at a known value, so we can then send a command to actuate all pins to a desired home position. Note that the actuating power for the calibration of the small actuators must be sufficiently low so that the actuators are not damaged when the pins are stopped when they hit the metal plate while the actuators are still active.

4.3 Grasping

In our experiments, a regular tetrahedron is used as a test object. Figure 10 and 11 show two grasps of this object. The desired configuration viewed from the top is shown in Figure 10(a) and 11(a). This target configuration is also marked on the lower plate to help verify the successful execution of the task. In Figure 10(b) and 11(b), the tetrahedron is placed in some arbitrary configuration in the vicinity of the target. When the corresponding

grasping operation is executed, we can see that the tetrahedron is moved to and immobilized at the target configuration (Figure 10(c) and 11(c)). Now we command the gripper to lift the top plate to the height associated with the maximum ICS of the grasp. We can verify that the tetrahedron is inescapable by trying to move it out of the capture. In this two example, we cannot take the tetrahedron out of the capture without bending the pins. Figure 10(d) and 11(d) show the most clockwise orientation in the capture, and Figure 10(e) and 11(e) show the most counterclockwise orientation in the capture. Trying to lower the top plate to the immobilizing height again from these extreme configurations, the tetrahedron again is immobilized exactly at the target configuration (Figure 10(f) and 11(f)).

4.4 In-Hand Manipulation

The first demonstration is a short manipulation sequence. See Figure 12. This manipulation has three steps and basically rotates the tetrahedron clockwise about 30 degrees. The targets for the three steps are marked on the board as shown in Figure 12(a). First, we place the tetrahedron in some configuration close to the target mark of the first step (Figure 12(b)) and execute the manipulation sequence. We can see that for each step in the sequence, the tetrahedron is successfully moved to the desired configuration (Figure 12(c)-(e)).

The second demonstration shows a longer manipulation sequence. This

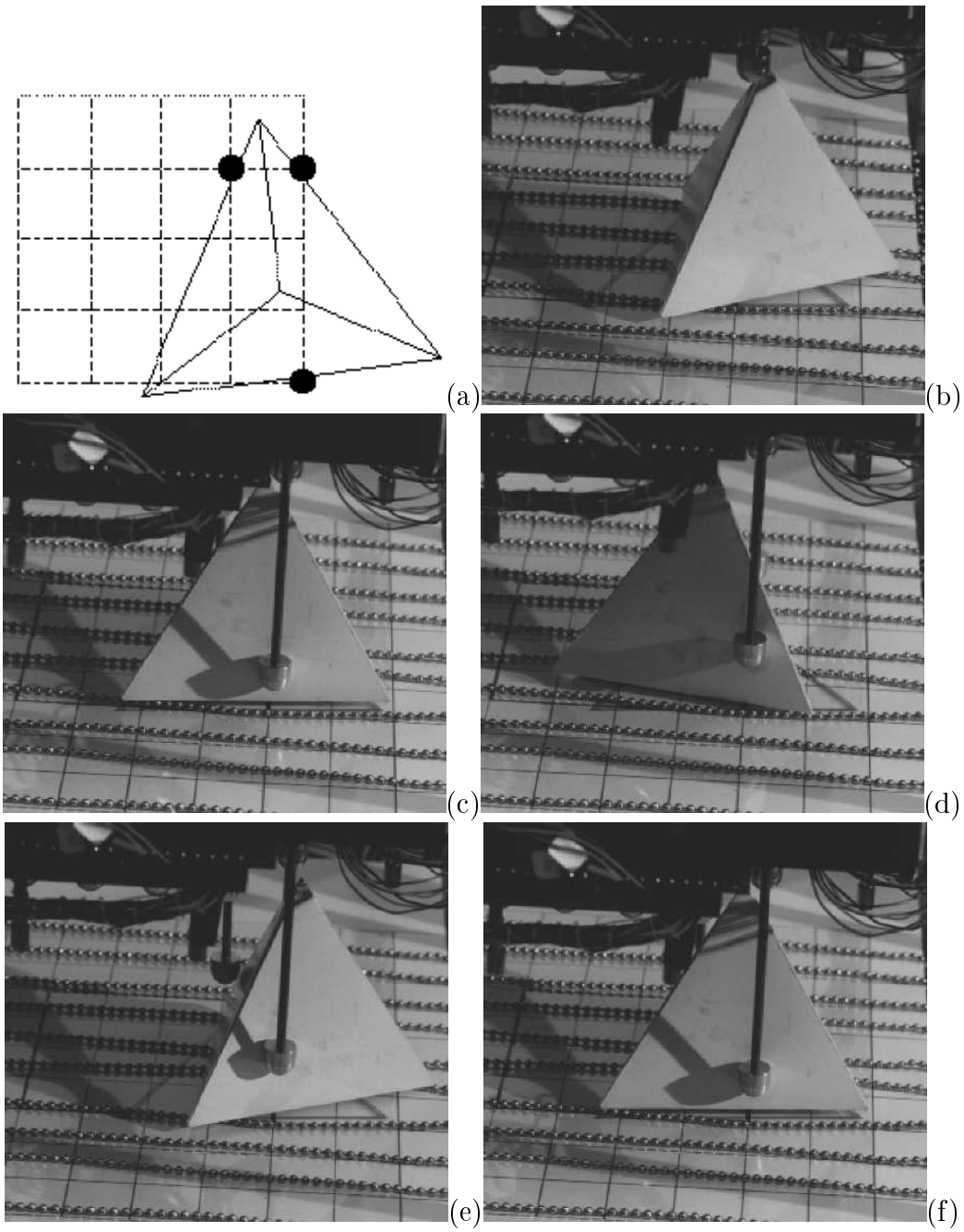

Figure 10: A grasp.

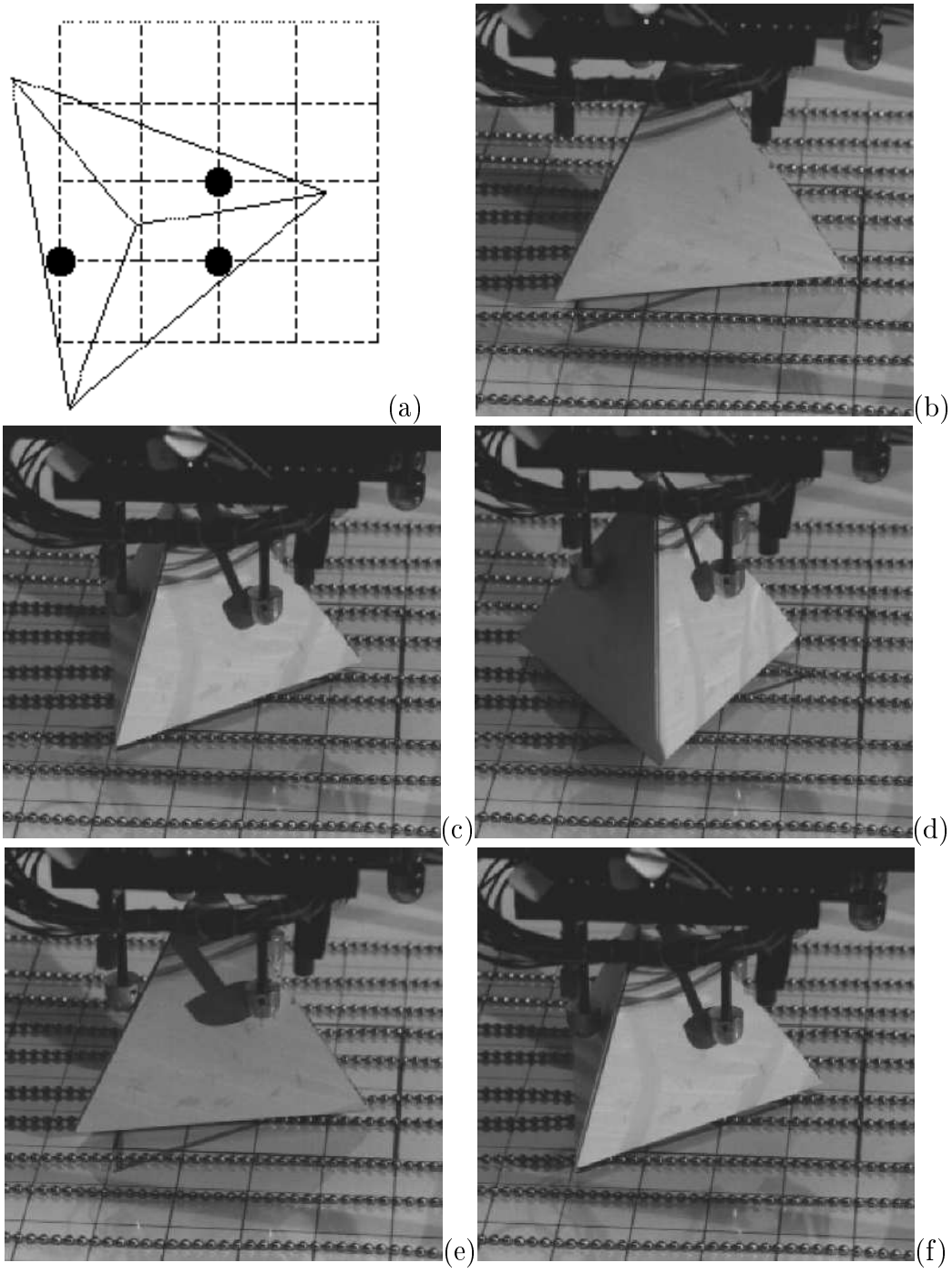

Figure 11: Another grasp.

sequence contains 39 manipulation steps. All steps are shown in Figure 13(a). In the illustration shown in Figure 14, the lower plate are marked with initial, final, and three intermediate configurations (Figure 13(b)). Again, as shown in Figure 14(c)-(e), the tetrahedron successfully reaches the final configuration when the manipulation sequence is executed.

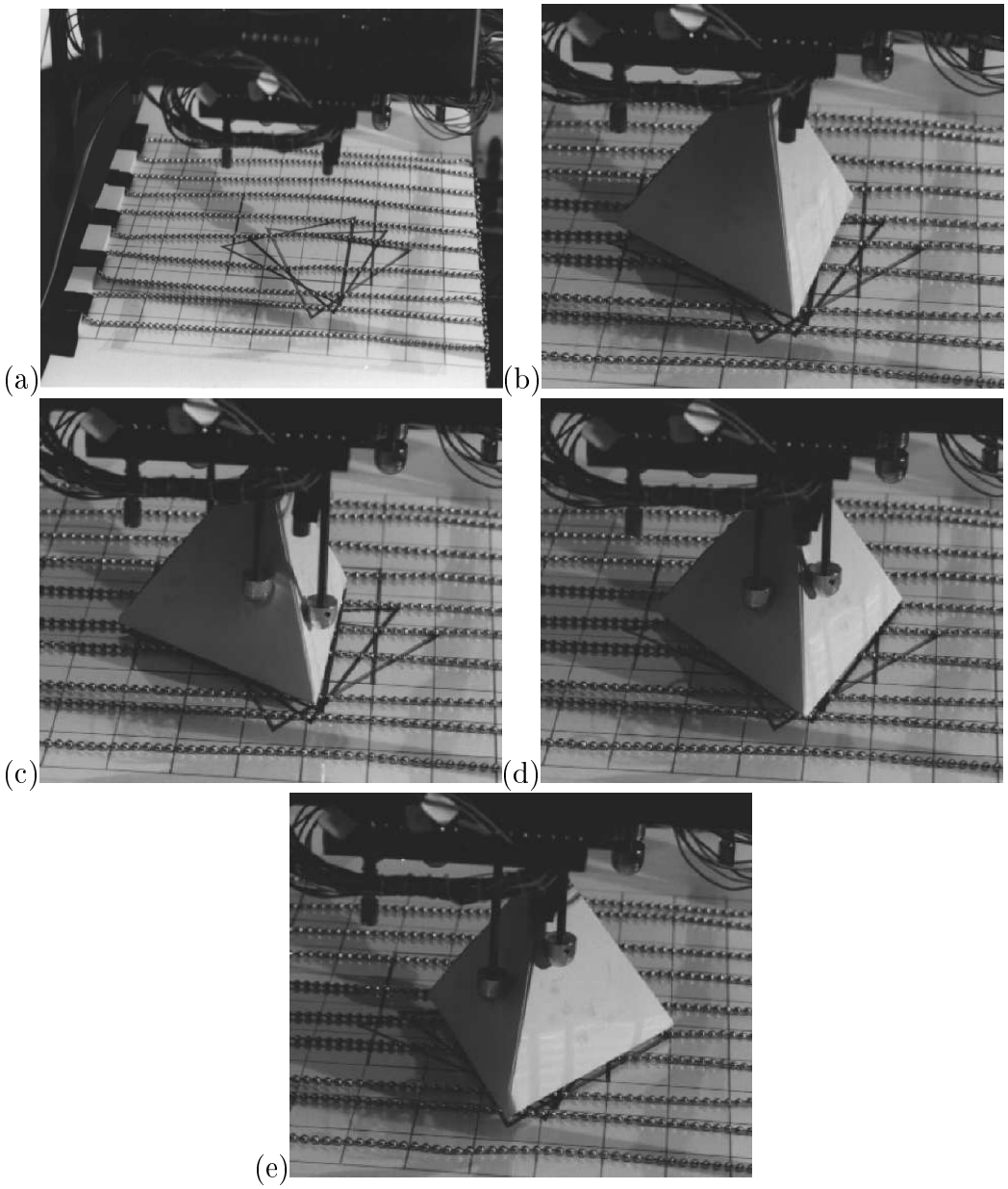

Figure 12: A short manipulation sequence.

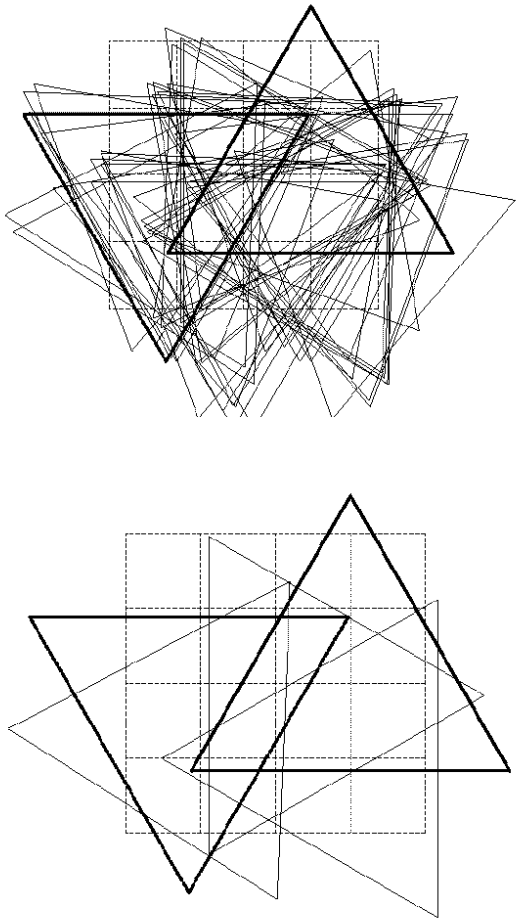

(b)

Figure 13: Steps in a manipulation.

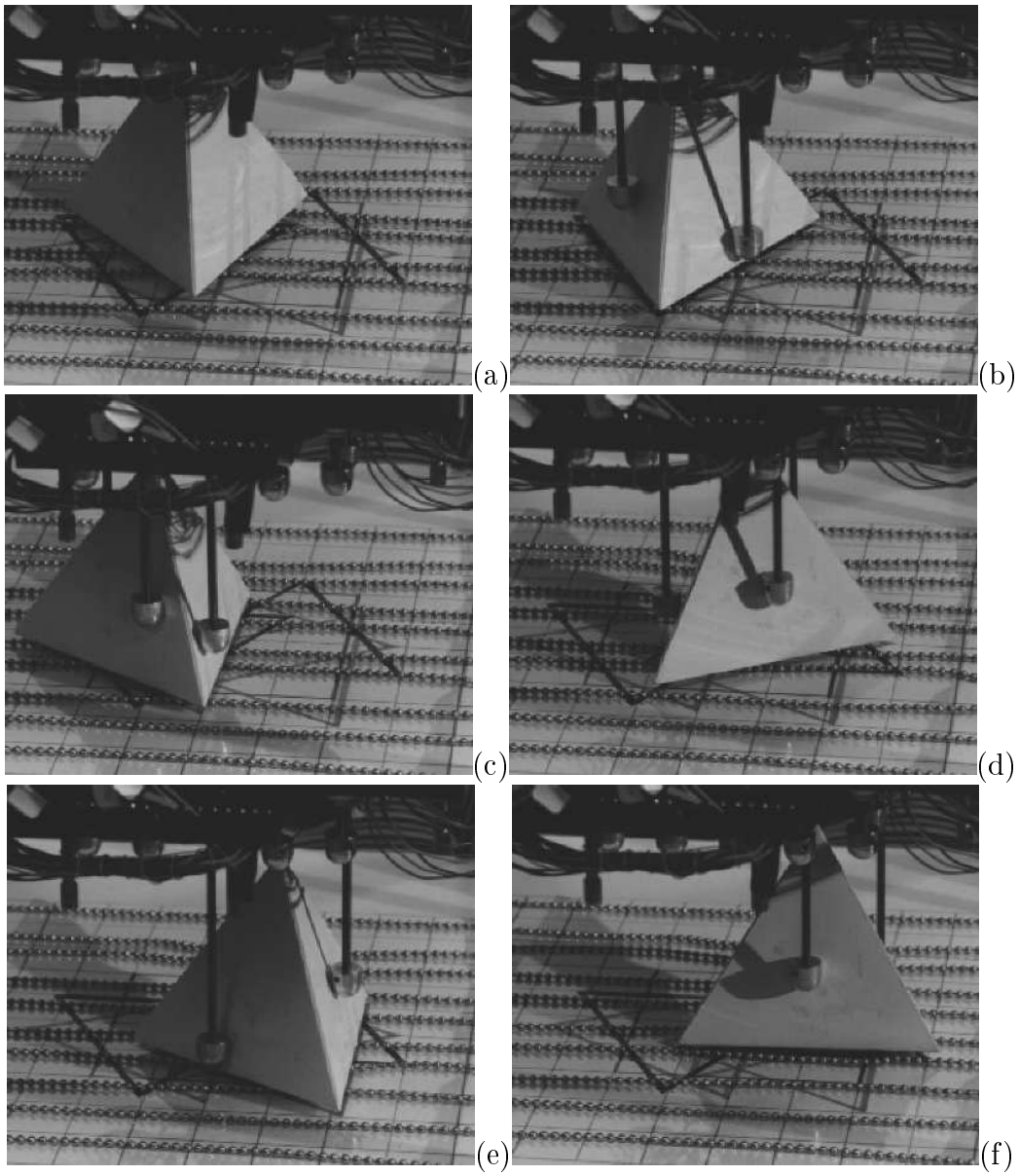

Figure 14: Another manipulation sequence.

5 Discussion

We have presented preliminary grasping and manipulation experiments with a prototype of a reconfigurable gripper. As mentioned earlier, our current prototype was only intended for these proof-of-concepts experiments. We now plan to construct a better-designed second-generation prototype, with much fewer actuators and higher accuracy and reliability.

We are investigating various extensions of our in-hand manipulation approach: for example, the stepper motors used to actuate the pins of our reconfigurable gripper allow essentially continuous vertical motions of the pins. We plan to address the problem of constructing manipulation plans that exploit these continuous degrees of freedom. We have recently extended our approach to the problem of manipulating a polygonal object with three disc-shaped robots in the plane [43] and hope to report actual experiments with Khepera miniature mobile robots soon.

Acknowledgments: This research was supported in part by the National Science Foundation under grant IRI-9634393, by a Critical Research Initiative planning grant from the University of Illinois at Urbana-Champaign, by an equipment grant from the Beckman Institute for Advanced Science and Technology, and by a grant from the Campus Research Board of the University of Illinois at Urbana-Champaign. N. Srinivasa was supported by a Beckman Fellowship. Part of this research was conducted while J. Ponce was

visiting the Department of Electrical Engineering and Computer Science of the University of California at Berkeley. We wish to thank Monique Teillaud, Olivier Devillers and David Hsu for useful discussions and comments.

References

[1] S. Akella and M.T. Mason. Parts orienting by push-aligning. In *IEEE Int. Conf. on Robotics and Automation*, pages 414–420, Nagoya, Japan, May 1995.

[2] R.S. Ball. *A treatise on the theory of screws.* Cambridge University Press, 1900.

[3] A. Blake. Computational modelling of hand-eye coordination. *Phil. Trans. R. Soc. Lond. B*, 337:351–360, 1992.

[4] R.C. Brost and K. Goldberg. A complete algorithm for synthesizing modular fixtures for polygonal parts. In *IEEE Int. Conf. on Robotics and Automation*, pages 535–542, San Diego, CA, May 1994.

[5] R.C. Brost and R.R. Peters. Automatic design of 3D fixtures and assembly pallets. In *IEEE Int. Conf. on Robotics and Automation*, pages 495–502, Minneapolis, MN, April 1996.

[6] J.F. Canny and K.Y. Goldberg. "RISC" for industrial robotics: recent results and open problems. In *IEEE Int. Conf. on Robotics and Automation*, pages 1951–1958, San Diego, CA, 1994.

[7] I.M. Chen and J.W. Burdick. Finding antipodal point grasps on irregularly shaped objects. In *IEEE Int. Conf. on Robotics and Automation*, pages 2278–2283, Nice, France, June 1992.

[8] J. Czyzowicz, I. Stojmenovic, and J. Urrutia. Immobilizing a polytope. volume 519 of *Lecture Notes in Computer Sciences*, pages 214–227. Springer-Verlag, 1991.

[9] M.A. Erdmann and M.T. Mason. An exploration of sensorless manipulation. *IEEE Journal of Robotics and Automation*, 4:369–379, 1988.

[10] C. Ferrari and J.F. Canny. Planning optimal grasps. In *IEEE Int. Conf. on Robotics and Automation*, pages 2290–2295, Nice, France, June 1992.

[11] J.B.J. Fourier. Reported in: Analyse des travaux de l'académie royale des sciences pendant l'année 1824. In *Partie mathématique, Histoire de l'Académie Royale des Sciences de l'Institut de France*, volume 7, xlvii-lv. 1827. Partial English translation in: D.A. Kohler, Translation of a Report by Fourier on his work on Linear Inequalities, *Opsearch* 10 (1973) 38-42.

[12] K.Y. Goldberg. Orienting polygonal parts without sensors. *Algorithmica*, 10(2):201–225, 1993.

[13] K.H. Hunt. *Kinematic Geometry of Mechanisms*. Clarendon, Oxford, 1978.

[14] K. Lakshminarayana. Mechanics of form closure. Technical Report 78-DET-32, ASME, 1978.

[15] C. Lassez and J-L. Lassez. Quantifier elimination for conjunctions of linear constraints via a convex hull algorithm. In B. Donald, D. Kapur, and J. Mundy, editors, *Symbolic and Numerical Computation for Artificial Intelligence*, pages 103–122. Academic Press, 1992.

[16] J-L. Lassez. Querying constraints. In *ACM conference on Principles of Database Systems*, Nashville, 1990.

[17] J.-C. Latombe. *Robot Motion Planning*. Kluwer Academic Publishers, 1991.

[18] K.M. Lynch and M.T. Mason. Stable pushing: mechanics, controllability, and planning. In K.Y. Goldberg, D. Halperin, J.-C. Latombe, and R. Wilson, editors, *Algorithmic Foundations of Robotics*, pages 239–262. A.K. Peters, 1995.

[19] X. Markenscoff and C.H. Papadimitriou. Optimum grip of a polygon. *International Journal of Robotics Research*, 8(2):17–29, April 1989.

[20] M.T. Mason. Mechanics and planning of manipulator pushing operations. *International Journal of Robotics Research*, 5(3):53–71, 1986.

[21] B. Mirtich and J.F. Canny. Optimum force-closure grasps. Technical Report ESRC 93-11/RAMP 93-5, Robotics, Automation, and Manufacturing Program, University of California at Berkeley, July 1993.

[22] B. Mishra. Worksholding – analysis and planning. In *IEEE/RSJ Int. Workshop on Intelligent Robots and Systems*, pages 53–56, Osaka, Japan, 1991.

[23] B. Mishra, J.T. Schwartz, and M. Sharir. On the existence and synthesis of multifinger positive grips. *Algorithmica, Special Issue: Robotics*, 2(4):541–558, November 1987.

[24] B. Mishra and N. Silver. Some discussion of static gripping and its stability. *IEEE Systems, Man, and Cybernetics*, 19(4):783–796, 1989.

[25] V-D. Nguyen. Constructing force-closure grasps. *International Journal of Robotics Research*, 7(3):3–16, June 1988.

[26] M.S. Ohwovoriole. An extension of screw theory. *Journal of Mechanical Design*, 103:725–735, 1981.

[27] N.S. Pollard and T. Lozano-Pérez. Grasp stability and feasibility for an arm with an articulated hand. In *IEEE Int. Conf. on Robotics and Automation*, pages 1581–1585, Cincinatti, OH, 1990.

[28] J. Ponce. On planning immobilizing fixtures for three-dimensional polyhedral objects. In *IEEE Int. Conf. on Robotics and Automation*, pages 509–514, Minneapolis, MN, April 1996.

[29] J. Ponce and B. Faverjon. On computing three-finger force-closure grasps of polygonal objects. *IEEE Transactions on Robotics and Automation*, 11(6):868–881, December 1995.

[30] J. Ponce, D. Stam, and B. Faverjon. On computing force-closure grasps of curved two-dimensional objects. *International Journal of Robotics Research*, 12(3):263–273, June 1993.

[31] J. Ponce, S. Sullivan, A. Sudsang, J-D. Boissonnat, and J-P. Merlet. On computing four-finger equilibrium and force-closure grasps of polyhedral objects. *International Journal of Robotics Research*, 16(1):11–35, February 1997.

[32] F.P. Preparata and M.I. Shamos. *Computational Geometry - An Introduction.* Springer-Verlag, 1985.

[33] A.S. Rao and K.Y. Goldberg. Manipulating algebraic parts in the plane. *IEEE Transactions on Robotics and Automation*, pages 598–602, 1995.

[34] F. Reulaux. *The kinematics of machinery.* MacMillan, NY, 1876. Reprint, Dover, NY, 1963.

[35] E. Rimon and A. Blake. Caging 2D bodies by one-parameter two-fingered gripping systems. In *IEEE Int. Conf. on Robotics and Automation*, pages 1458–1464, Minneapolis, MN, April 1996.

[36] E. Rimon and J. W. Burdick. Towards planning with force constraints: On the mobility of bodies in contact. In *Proc. IEEE Int. Conf. on Robotics and Automation*, pages 994–1000, Atlanta, GA, May 1993.

[37] E. Rimon and J. W. Burdick. Mobility of bodies in contact-I: A new 2^{nd} order mobility index for multi-finger grasps. *IEEE Transactions on Robotics and Automation*, 1995. Submitted. A preliminary version appeared in *IEEE Int. Conf. on Robotics and Automation*, pages 2329-2335, San Diego, CA, 1994.

[38] E. Rimon and J. W. Burdick. Mobility of bodies in contact-II: How forces are generated by curvature effects? *IEEE Transactions on Robotics and Automation*, 1995. Submitted. A preliminary version appeared in *IEEE Int. Conf. on Robotics and Automation*, pages 2336-2341, San Diego, CA, 1994.

[39] B. Roth. Screws, motors, and wrenches that cannot be bought in a hardware store. In *Int. Symp. on Robotics Research*, pages 679–693. MIT Press, 1984.

[40] J.K. Salisbury. *Kinematic and force analysis of articulated hands*. PhD thesis, Stanford University, Stanford, CA, 1982.

[41] P. Somov. Über Gebiete von Schraubengeschwindigkeiten eines starren Korpers bie verschiedener Zahl von Stutzflachen. *Zeitricht für Mathematik und Physik*, 45:245–306, 1900.

[42] A. Sudsang and J. Ponce. In-hand manipulation: geometry and algorithms. In *IEEE/RSJ International Conference on Intelligent Robots and Systems*, pages 98–105, Grenoble, France, September 1997.

[43] A. Sudsang and J. Ponce. On grasping and manipulating polygonal objects with disc-shaped robots in the plane. In *IEEE Int. Conf. on Robotics and Automation*, 1998. Submitted.

[44] A. Sudsang, J. Ponce, and N. Srinivasa. Grasping and in-hand manipulation: Geometry and algorithms. *Algorithmica*, 1997.

[45] A. Sudsang, N. Srinivasa, and J. Ponce. On planning immobilizing grasps for a reconfigurable gripper. In *IEEE/RSJ International Conference on Intelligent Robots and Systems*, pages 106–113, Grenoble, France, September 1997.

[46] R. Wagner, Y. Zhuang, and K. Goldberg. Fixturing faceted parts with seven modular struts. In *IEEE Int. Symp. on Assembly and Task Planning*, pages 133–139, Pittsburgh, PA, August 1995.

[47] A. Wallack and J.F. Canny. Planning for modular and hybrid fixtures. In *IEEE Int. Conf. on Robotics and Automation*, pages 520–527, San Diego, CA, 1994.

[48] A.S. Wallack. *Algorithms and Techniques for Manufacturing.* PhD thesis, Computer Science Division, Univ. of California at Berkeley, 1995.